

Multiple Orientation of Melittin inside a Single Lipid Bilayer Determined by Combined Vibrational Spectroscopic Studies

Xiaoyun Chen, Jie Wang, Andrew P. Boughton, Cornelius B. Kristalyn,
and Zhan Chen*

Contribution from the Department of Chemistry, University of Michigan,
Ann Arbor, Michigan 48109

Received October 20, 2006; E-mail: zhanc@umich.edu

Abstract: Despite the availability of several mature structure determination techniques for bulk proteins, determination of structural and orientational information of interfacial proteins, e.g., in cell membranes or on biomaterial surfaces, remains a difficult problem. We combine sum frequency generation (SFG) vibrational spectroscopy with attenuated total reflection-Fourier transform infrared spectroscopy (ATR-FTIR) to investigate the orientation of α -helical peptides reconstituted in substrate supported lipid bilayers. Melittin was chosen as a model for α -helical peptides, and its orientation when interacting with a supported 1,2-dipalmitoyl-*sn*-glycero-3-phosphoglycerol (DPPG) bilayer has been examined. Through polarization analysis using amide I signals obtained from both SFG and ATR-FTIR measurements, the orientation distribution of melittin inside a DPPG bilayer was deduced using several trial distribution functions. Melittin was modeled as either an ideal helix or a helix with a bent structure. It was found that a simple distribution function such as a δ -distribution or a Gaussian distribution was not adequate to describe the melittin orientation distribution inside a DPPG bilayer. Instead, two populations of melittin, corresponding to two melittin-bilayer association states, could be used to interpret the experimentally observed result. The method employed in this study demonstrates the feasibility of acquiring a more accurate orientation distribution of peptides/proteins in situ using a combination of vibrational spectroscopic techniques without exogenous labeling.

Proteins carry out or mediate numerous cellular activities at interfaces: cell motility, signal transduction, vesicular transportation including vesicle budding and fusion, and the creation of cross-membrane potential, etc. Structure determination of these proteins is vital to understanding their function, which in turn can lead to rational design of molecules that can more effectively mediate or interfere with the above-mentioned cellular events in the desired manner. Currently, the biggest hurdle in elucidating the structures of interfacial proteins is a lack of suitable techniques that can specifically probe interfacial protein structures. Taking membrane protein structure determination as an example, except for a few microscopic techniques, samples are often composed of proteins intercalated within multi-bilayers or solubilized inside non-native protein-detergent complexes.^{1–3} Recently, SFG has been widely used to study interfacial structures of complex molecules, including proteins.^{4–15}

Our lab has been developing nonlinear optical spectroscopic techniques, especially sum frequency generation (SFG) vibrational spectroscopy, for the investigation of interfacial protein structure. We have demonstrated that SFG signals can be observed from both the protein C–H and C=O vibrational modes and that SFG can distinguish between different secondary structures.^{16,17} In this paper, we will demonstrate the analysis of SFG amide I signals of proteins to deduce orientation of α -helices, using results obtained from the α -helical model peptide melittin. The methodology for orientation analysis described in this paper is also being applied to other secondary structures and should lead to more accurate interfacial protein structure determination in situ without exogenous labeling.

Melittin is naturally found in bee venom toxin. It is composed of 26 amino acid residues and is highly positively charged in physiological conditions.¹⁸ It has been extensively studied in an effort to understand how peptide interacts with cell membrane

- (1) Engel, A. *Histochem. Cell Biol.* **2003**, *120*, 93–102.
- (2) Opella, S. J.; Marassi, F. M. *Chem. Rev.* **2004**, *104*, 3587–3606.
- (3) Wiener, M. C. *Methods* **2004**, *34*, 364–372.
- (4) Kim, J.; Somorjai, G. A. *J. Am. Chem. Soc.* **2003**, *125*, 3150–3158.
- (5) Mermut, O.; Phillips, D. C.; York, R. L.; McCrear, K. R.; Ward, R. S.; Somorjai, G. A. *J. Am. Chem. Soc.* **2006**, *128*, 3598–3607.
- (6) Jung, S. Y.; Lim, S. M.; Albertorio, F.; Kim, G.; Gurau, M. C.; Yang, R. D.; Holden, M. A.; Cremer, P. S. *J. Am. Chem. Soc.* **2003**, *125*, 12782–12786.
- (7) Dreesen, L.; Humbert, C.; Sartenaer, Y.; Caudano, Y.; Volcke, C.; Mani, A. A.; Peremans, A.; Thiry, P. A.; Hanique, S.; Frere, J. M. *Langmuir* **2004**, *20*, 7201–7207.
- (8) Dreesen, L.; Sartenaer, Y.; Humbert, C.; Mani, A. A.; Methivier, C.; Pradier, C. M.; Thiry, P. A.; Peremans, A. *ChemPhysChem* **2004**, *5*, 1719–1725.
- (9) Ma, G.; Allen, H. C. *Langmuir* **2006**, *22*, 5341–5349.

- (10) Holman, J.; Davies, P. B.; Nishida, T.; Ye, S.; Neivandt, D. J. *J. Phys. Chem. B* **2005**, *109*, 18723–18732.
- (11) Watry, M. R.; Richmond, G. L. *Langmuir* **2002**, *18*, 8881–8887.
- (12) Ye, S.; Noda, H.; Nishida, T.; Morita, S.; Osawa, M. *Langmuir* **2004**, *20*, 357–365.
- (13) Liu, J.; Conboy, J. C. *Biophys. J.* **2005**, *89*, 2522–2532.
- (14) Wang, J.; Buck, S. M.; Chen, Z. *Analyst* **2003**, *128*, 773–778.
- (15) Wang, J.; Clarke, M. L.; Zhang, Y. B.; Chen, X.; Chen, Z. *Langmuir* **2003**, *19*, 7862–7866.
- (16) Wang, J.; Even, M. A.; Chen, X.; Schmaier, A. H.; Waite, J. H.; Chen, Z. *J. Am. Chem. Soc.* **2003**, *125*, 9914–9915.
- (17) Chen, X.; Wang, J.; Sniadecki, J. J.; Even, M. A.; Chen, Z. *Langmuir* **2005**, *21*, 2662–2664.
- (18) Dempsey, C. E. *Biochim. Biophys. Acta* **1990**, *1031*, 143–161.

bilayers. Melittin is shown to have a random structure in aqueous solution but adopts an α -helical structure when adsorbing onto a lipid bilayer.^{18–20} The orientation of melittin helices inside a lipid bilayer thus naturally become the most important parameter to be determined in order to gain a molecular level understanding of the mode of interaction of melittin with a bilayer. Through many previous studies employing various biophysical techniques, it is now known that melittin can exist in two states when interacting with a lipid bilayer: the surface associated state, with the helical axis more or less parallel to the bilayer surface, and the inserted state, with the helical axis more or less perpendicular to the bilayer surface.^{21–28} It has been proposed that there is a surface threshold concentration above which melittin can change from the membrane surface-associated state to the inserted state. However, many details regarding melittin orientation remain unclear. Several different experimental systems have been used in previous investigations of melittin/bilayer interactions. In one typical system, melittin and lipids are premixed in a cosolvent, such as chloroform, and dried. The resultant powder is then rehydrated to form a multi-bilayer/melittin system. In another type of experiment, a supported bilayer is preformed and then allowed to interact with melittin that is injected into the aqueous phase.²⁸ While the former system may represent a thermally favorable equilibrium system, the second system may offer a more biologically relevant condition for melittin to adsorb and interact with a bilayer. In addition, information about the kinetics of interaction can only be obtained from the latter type of system. Therefore, in this work, we will examine the melittin orientation during its interaction with a DPPG bilayer using the latter type of system.

SFG and ATR-FTIR amide I signals will be utilized in this paper to deduce the melittin orientation in a lipid bilayer. Past research using ATR-FTIR has shown that amide I bands of peptides/proteins are sensitive to not only conformation but also orientation of proteins.^{29–32} There have been many examples of the use of ATR-FTIR to determine protein/peptide orientation inside membrane bilayers. The axial symmetry of an α -helix allows us to use one parameter, θ , the tilt angle between the membrane surface normal and the principal axis of the helix, to describe the orientation. In ATR-FTIR studies, the ensemble average of the tilt angle $\langle \cos^2 \theta \rangle$ can be determined from the measured dichroic ratio and is often represented by the order parameter $S_\theta = (3\langle \cos^2 \theta \rangle - 1)/2$, with $S_\theta = 1$ representing helices orientated perpendicularly to the surface and $S_\theta = -0.5$ representing helices lying down parallel to the surface. For most

biological samples, however, S_θ is between -0.5 and 1 , and there can be ambiguity as to the exact orientation of helices. For example, when S_θ is equal to 0 , $\langle \cos^2 \theta \rangle$ is equal to $1/3$, and this can correspond to either a δ -distribution of $\theta = 54.7^\circ$ or a completely random distribution of helix orientation, or many combinations of orientations and distributions in between. For α -helices, SFG can be used to measure two additional independent parameters, $\langle \cos \theta \rangle$ and $\langle \cos^3 \theta \rangle$, and thus greatly reduce the ambiguity involved. Past research has determined the distribution function for methyl group orientation on polymer surfaces based on Gaussian distributions from these two measurements.^{33–35} Here we will demonstrate that more details regarding α -helical peptide orientation in lipid bilayers in situ can be extracted from polarization analysis when we combine the SFG and ATR-FTIR measurements. We believe that such detailed orientational information cannot be observed using other analytical techniques, or ATR-FTIR or SFG alone.

Currently many antimicrobial peptides are being investigated as candidates to overcome the resistance that bacteria have developed to conventional antibiotics.³⁶ The results obtained from these studies provide molecular insight regarding antimicrobial peptide–cell membrane interactions, which are closely related to peptide orientation in cell membranes. Such information can thus aid in developing antimicrobial peptides with improved performance. Furthermore, the deduction of orientation distributions of α -helices of model peptides will serve as a basis for future investigation of proteins with more complicated structures, a classic example being G-protein coupled receptors with seven transmembrane helical domains.

Theoretical Background

Polarization Analysis for Orientation Deduction. In a typical SFG experiment, a visible beam and a tunable IR beam are overlapped spatially and temporally at interfaces of interest. A third beam at the sum frequency of the two incident beams is then generated and monitored as a function of IR frequency. When the IR frequency is resonant with molecular vibrational modes, the SFG beam intensity can be enhanced. An SFG spectrum is obtained by plotting the SFG intensity against IR frequency. The general theory relating SFG signal intensity to surface second-order nonlinear optical susceptibility $\chi^{(2)}$ and to molecular hyperpolarizability $\beta^{(2)}$ has been thoroughly described and will not be repeated here.^{37–41} Discussion below will focus on how orientation information of interfacial helices can be deduced from SFG amide I signals, which have only been observed and studied recently.

In order to deduce the orientation of α -helices from SFG signals obtained using various polarization combinations, we need to know how $\chi^{(2)}$, the second-order surface susceptibility of interfacial peptides in the lab coordinate system, is related to $\beta^{(2)}$, the hyperpolarizability of an α -helix in the molecular coordinate system. In a recent study employing normal-mode analysis, we have shown that both the A mode

(19) Terwilliger, T. C.; Eisenberg, D. *J. Biol. Chem.* **1982**, *257*, 6010–6015.

(20) Terwilliger, T. C.; Eisenberg, D. *J. Biol. Chem.* **1982**, *257*, 6016–6022.

(21) Allende, D.; Simon, S. A.; McIntosh, T. J. *Biophys. J.* **2005**, *88*, 1828–1837.

(22) Constantinescu, I.; Laffleur, M. *Biochim. Biophys. Acta, Biomembranes* **2004**, *1667*, 26–37.

(23) Toraya, S.; Nishimura, K.; Naito, A. *Biophys. J.* **2004**, *87*, 3323–3335.

(24) Hristova, K.; Dempsey, C. E.; White, S. H. *Biophys. J.* **2001**, *80*, 801–811.

(25) Ladokhin, A. S.; White, S. H. *Biochim. Biophys. Acta* **2001**, *1514*, 253–260.

(26) Yang, L.; Harroun, T. A.; Weiss, T. M.; Ding, L.; Huang, H. W. *Biophys. J.* **2001**, *81*, 1475–1485.

(27) Steinem, C.; Galla, H.; Janshoff, A. *Phys. Chem. Chem. Phys.* **2000**, *2*, 4580–4585.

(28) Frey, S.; Tamm, L. K. *Biophys. J.* **1991**, *60*, 922–930.

(29) Tamm, L. K.; Tatulian, S. A. *Q. Rev. Biophys.* **1997**, *30*, 365–429.

(30) Barth, A.; Zscherp, C. *Q. Rev. Biophys.* **2002**, *35*, 369–430.

(31) Goormaghtigh, E.; Raussens, V.; Ruysschaert, J. *Biochim. Biophys. Acta, Reviews on Biomembranes* **1999**, *1422*, 105–185.

(32) Tatulian, S. A. *Biochemistry* **2003**, *42*, 11898–11907.

(33) Wang, J.; Paszti, Z.; Even, M. A.; Chen, Z. *J. Am. Chem. Soc.* **2002**, *124*, 7016–7023.

(34) Wang, J.; Lee, S.; Chen, Z., intended to be submitted.

(35) Wang, J.; Paszti, Z.; Clarke, M. L.; Chen, X.; Chen, Z., intended to be submitted.

(36) Zasloff, M. *Nature* **2002**, *415*, 389–395.

(37) Shen, Y. R. *The Principles of Nonlinear Optics*; J. Wiley: New York, 1984.

(38) Hirose, C.; Akamatsu, N.; Domen, K. *J. Chem. Phys.* **1992**, *96*, 997–1004.

(39) Zhuang, X.; Miranda, P. B.; Kim, D.; Shen, Y. R. *Phys. Rev. B* **1999**, *59*, 12632–12640.

(40) Wei, X.; Hong, S. C.; Zhuang, X. W.; Goto, T.; Shen, Y. R. *Phys. Rev. E* **2000**, *62*, 5160–5172.

(41) Wang, J.; Chen, C. Y.; Buck, S. M.; Chen, Z. *J. Phys. Chem. B* **2001**, *105*, 12118–12125.

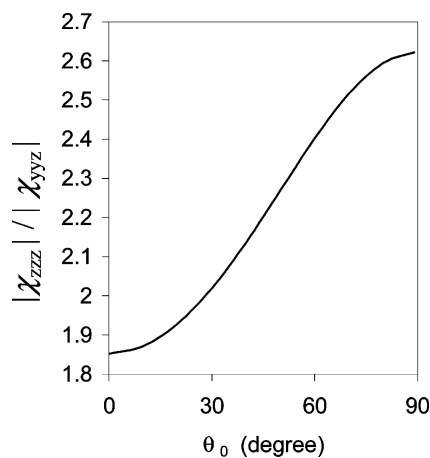


Figure 1. $|\chi_{zzz}/\chi_{yyz}|$ ratio as a function of orientation angle θ_0 , assuming a δ -distribution.

and E_1 mode of α -helix amide I stretching can contribute SFG signals.³⁴ The hyperpolarizability of an α -helix can be obtained from the product of the Raman polarizability derivative and IR dipole moment derivative. Using the near total internal reflection geometry,¹⁶ ssp (s-polarized SFG output, s-polarized visible input, and p-polarized IR input) and ppp amide I signals are mainly contributed by χ_{yyz} and χ_{zzz} susceptibility components, respectively, and their dependence on molecular hyperpolarizability is described by the following equations (superscript ⁽²⁾ omitted in text for simplicity from here on):

For the A mode,

$$\chi_{A,xxz} = \chi_{A,yyz} = \frac{1}{2}N_s[(1+r)\langle\cos\theta\rangle - (1-r)\langle\cos^3\theta\rangle]\beta_{ccc} \quad (1)$$

$$\chi_{A,zzz} = N_s[r\langle\cos\theta\rangle + (1-r)\langle\cos^3\theta\rangle]\beta_{ccc} \quad (2)$$

For the E_1 mode,

$$\chi_{E_1,xxz} = \chi_{E_1,yyz} = -N_s(\langle\cos\theta\rangle - \langle\cos^3\theta\rangle)\beta_{aca} \quad (3)$$

$$\chi_{E_1,zzz} = 2N_s(\langle\cos\theta\rangle - \langle\cos^3\theta\rangle)\beta_{aca} \quad (4)$$

where β_{aca} and β_{ccc} are the molecular hyperpolarizability elements with the following relationship $\beta_{aca} \approx 0.32\beta_{ccc}$. The depolarization ratio r has the value $\beta_{aac}/\beta_{ccc} \approx 0.54$.^{42–45} N_s is the number density of ideal α -helix units composed of 18 amino acid residues. Therefore it is necessary to include a scaling factor N_p/N_s for α -helical peptides with N_p amino acid residues in the helical domain. For melittin, $N_p = 26$. Since the A mode and E_1 mode cannot be readily resolved in the frequency domain with our system's resolution, we will assume that the total susceptibility is simply a sum of susceptibilities from these two modes.

$$\chi_{yyz} = \chi_{A,yyz} + \chi_{E_1,yyz} \quad (5)$$

$$\chi_{zzz} = \chi_{A,zzz} + \chi_{E_1,zzz} \quad (6)$$

From the above derivation, it can be seen that $|\chi_{zzz}/\chi_{yyz}|$ of SFG amide I signals from the helix changes monotonically as the helix tilt angle changes from 0° to 90° , as shown in Figure 1 (assuming a δ -orientation distribution of all helices). Therefore the phase of the amide I signals can also be determined (e.g., by interfering with resonant signals or

nonresonant background of a known phase) and then the absolute orientation of an ideal helix can be readily determined.

SFG Hyperpolarizability of a Bent Helix. While almost all of the 26 amino acids in the melittin sequence can be considered to possess α -helical structure, the bend caused by Pro¹⁴ may result in a significant deviation of melittin from an ideal helix. To account for the bent structure of melittin, we represent melittin as being composed of two α -helices, with an interhelical angle θ_h between the N-terminal helix segment and the C-terminal helix segment. It should be noted that a distribution function derived without considering such a bent structure may be able to capture the orientation distribution of both helices, as will be discussed later. To deduce the second-order susceptibility of a bent helix in the xyz lab coordinate system as shown in Figure 2b, we first derive the hyperpolarizability of the tilted C-terminus helix in the $x'y'z'$ molecular coordinate. As shown in Figure 2a, the C-terminus helix axis lies in the $x'-z'$ plane and tilts at an angle θ_h versus z' . After Euler transformation (same convention as that used in ref 46) setting θ to interhelical angle θ_h , ϕ to 0° and averaging ψ over 0° to 360° , and after considering the equality relationships for an α -helix $|\partial\mu_a/\partial Q| = |\partial\mu_b/\partial Q|$, $|\partial\alpha_{ac}/\partial Q| = |\partial\alpha_{bc}/\partial Q|$, all 27 SFG hyperpolarizability tensor elements for the tilted C-terminus helix segment (β_i) can be obtained for the A mode and the E_1 mode, among which 10 are nonzero for the A mode and 12 are nonzero for the E_1 mode. The residue-number weighted sum of β_i and hyperpolarizability tensor elements of the straight N-terminus helix segment (β_s) are the total hyperpolarizability (β_m) of a bent melittin as a unit.

The hyperpolarizability thus obtained can then be projected onto the surface coordinate assuming azimuthal symmetry by averaging over ϕ . It should be noticed that the averaging over twist angle that is commonly used for methyl groups can no longer be performed here due to the broken symmetry caused by the bent structure. The final form of χ is thus a function of both ψ and θ . Similar deduction of molecular hyperpolarizabilities for complex functional groups based on molecular geometry has also been performed for methyl groups in several recent publications.^{47–49}

Orientation Distribution Function. Except under rare conditions most interfacial biological molecules are dynamic and flexible in their native environment and their orientation should be described using orientation distribution functions. One way to determine protein orientation distribution functions is to study how proteins interact with polarized light. Polarized ATR-FTIR has been widely used to study orientation of membrane peptides/proteins. The order parameter obtained based on α -helix amide I modes can qualitatively describe whether helices orientate parallel or perpendicular to the bilayer surface. Fundamentally the order parameter is related to $\langle\cos^2\theta\rangle$, with θ being the tilt angle of helices and brackets denoting time and ensemble averaging. Due to the limited number of measurables in ATR-FTIR experiments, only the simplest distribution function can be determined, e.g., a δ -distribution, when all the helices at the interface adopt the same orientation. Under many conditions not all the helices adopt the same orientation; thus more parameters are needed to sufficiently characterize the orientation, and ATR-FTIR measurement alone is not adequate. For example, when the parameter S approaches 0, there is always ambiguity in whether all helices have the same tilt angle around 54.7° or are completely randomly oriented or other orientations/distributions in between. One effective way to reduce such ambiguity is to measure more parameters experimentally. As shown in eqs 1–6, SFG can measure $\langle\cos\theta\rangle$ and $\langle\cos^3\theta\rangle$. By investigating the same system with a combination of SFG and ATR-FTIR, we therefore can obtain three measurables, allowing the determination of more sophisticated

(42) Lee, S.; Krimm, S. *Biopolymers* **1998**, *46*, 283–317.

(43) Lee, S.; Krimm, S. *J. Raman Spectrosc.* **1998**, *29*, 73–80.

(44) Marsh, D.; Muller, M.; Schmitt, F. J. *Biophys. J.* **2000**, *78*, 2499–2510.

(45) Rintoul, L.; Carter, E. A.; Stewart, S. D.; Fredericks, P. M. *Biopolymers* **2000**, *57*, 19–28.

(46) Moad, A. J.; Simpson, G. J. *J. Phys. Chem. B* **2004**, *108*, 3548–3562.

(47) Chen, X.; Tang, H.; Even, M. A.; Wang, J.; Tew, G. N.; Chen, Z. *J. Am. Chem. Soc.* **2006**, *128*, 2711–2714.

(48) Kataoka, S.; Cremer, P. S. *J. Am. Chem. Soc.* **2006**, *128*, 5516–5522.

(49) Beattie, D. A.; Fraenkel, R.; Winget, S. A.; Petersen, A.; Bain, C. D. *J. Phys. Chem. B* **2006**, *110*, 2278–2292.

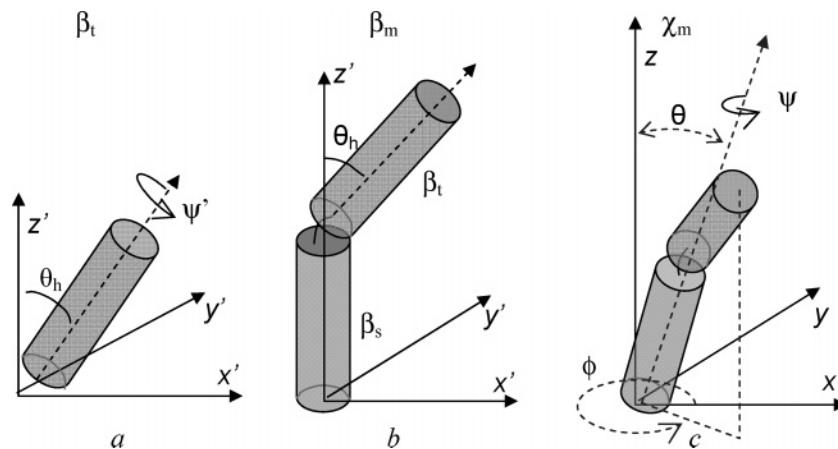


Figure 2. Derivation of molecular hyperpolarizability and surface susceptibility of melittin modeled as a bent helix.

orientation distribution functions. Though combining even higher order nonlinear optical spectroscopy may lead to even more accurate orientation determination, here we will focus on deducing the orientation distribution functions adopted by melittin inside a lipid bilayer from the three measured parameters $\langle \cos \theta \rangle$, $\langle \cos^2 \theta \rangle$, and $\langle \cos^3 \theta \rangle$ using SFG and ATR-FTIR.

With the three measurables available, a distribution function with a maximum of three parameters can theoretically be determined. Several trial distribution functions as described below will be calculated based on these parameters and evaluated. If we simplify melittin as having an ideal straight α -helical structure without considering the bend, only the distribution function of the tilt angle θ needs to be determined. The simplest distribution function is a δ -function, which requires the determination of only one parameter, the tilt angle. As mentioned before, a δ -function describes the situation where all the melittin molecules orient at the same angle versus the bilayer surface normal. The Gaussian function $(1/\sigma\sqrt{2\pi}) \exp(-(\theta - \theta_0)^2/2\sigma^2)$ has been extensively used to study orientation distribution, which requires the determination of two parameters: both the mean tilt angle θ_0 and the distribution width σ . In the following, the above-mentioned δ -distribution and Gaussian function will be used to characterize melittin orientation in our SFG and ATR-FTIR studies. It has been shown via other methods that, at different melittin concentrations, two different association states of melittin in cell membranes with different orientations can be observed. Therefore in this research a dual- δ -function will be the third trial distribution function to be tested, describing the situation in which melittin can adopt two orientations inside a bilayer. Besides two orientation angles θ_1 and θ_2 , an additional parameter, N , related to the number of melittin molecules adopting each orientation is required, so that $100N$ percent of melittin molecules orient at angle θ_1 , while the rest, $100(1 - N)$ percent, of the melittin molecules orient at angle θ_2 . It should be noted that the choice of a particular form of distribution function is fundamentally arbitrary and may not reflect the true orientation distribution melittin molecules adopted. Information theory has shown that maximum entropy theory offers the least biased approach in deducing orientation distribution based on limited measurables.⁵⁰ We therefore will also apply the maximum entropy function to analyze our SFG and ATR-FTIR results.

As mentioned above, in order to consider the bent structure of melittin, we will need to determine the orientation distribution functions for both θ and ψ . With three measured parameters, this can be achieved only by assuming δ -functions for both θ and ψ . We can no longer determine the parameters for other forms of distribution functions because more than three parameters will be required. Certainly in this case more measured parameters can be obtained in SFG studies, but

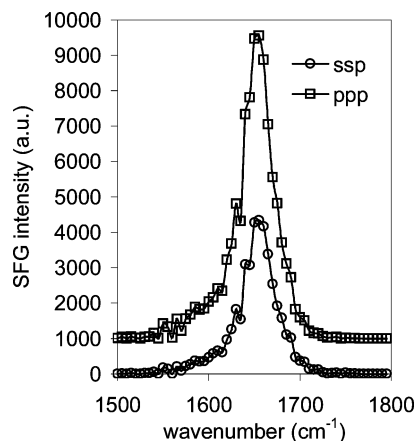


Figure 3. SFG amide I spectra collected from melittin adsorbed onto a DPPG supported bilayer at ssp and ppp polarization combination. A solution concentration of $0.78 \mu\text{M}$ is used. (a.u.: arbitrary unit.)

such data analysis is beyond the scope of this article and will not be discussed here. Theoretically if enough parameters can be measured, the maximum entropy function applied should lead to a correct distribution function.

Results and Discussion

SFG and ATR-FTIR Amide I Spectra. A melittin solution concentration of $0.78 \mu\text{M}$ is achieved by injecting about $5 \mu\text{L}$ of 0.8 mg/mL stock melittin solution into the subphase ($\sim 1.8 \text{ mL}$) of a supported bilayer. The reason for choosing this concentration is that, at higher melittin solution concentrations than this, significant lipid displacement from the support bilayer can be observed from ATR-FTIR, indicated by a decrease in lipid CH_2 absorbance around 2850 cm^{-1} and 2920 cm^{-1} . For solution concentrations lower than this, the amide I absorbance of melittin in ATR-FTIR is too weak to yield an adequate signal-to-noise ratio. The bilayer response deduced based on C-H/C-D stretching modes in another study also indicates that $0.78 \mu\text{M}$ is a critical concentration for melittin/DPPG bilayer interactions.⁵¹

Shown in Figure 3 are the SFG amide I spectra collected from interfacial melittin adsorbed onto a DPPG/DPPG bilayer using ssp and ppp polarization combinations. Amide I bands

(50) Mead, L. R.; Papanicolaou, N. *J. Math. Phys.* **1984**, *25*, 2404–2417.

(51) Chen, X.; Wang, J.; Kristalyn, C. B.; Chen, Z. *Biophys. J.*, submitted.

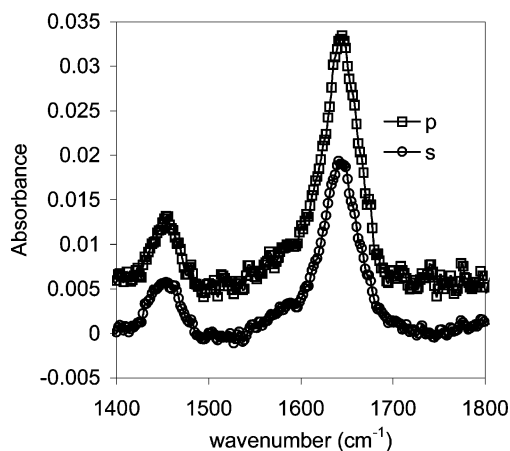


Figure 4. ATR-FTIR amide I spectra collected from melittin adsorbed onto a DPPG supported bilayer with p and s polarized IR. A solution concentration of $0.78 \mu\text{M}$ is used.

are the only dominant features between 1500 cm^{-1} and 1800 cm^{-1} in Figure 3. No amide II bands are observed, and lipid C=O stretching signals ($\sim 1720 \text{ cm}^{-1}$) are negligibly weak compared to melittin amide I bands. The amide I peak is centered around 1655 cm^{-1} , confirming that membrane-associated melittin indeed adopts an α -helical structure (Supporting Information). Spectral features remain essentially the same for ssp and ppp spectra, while the ppp spectral intensity at 1655 cm^{-1} is about two times stronger than that of the ssp spectrum.

Figure 4 displays ATR-FTIR spectra of melittin adsorbed onto a bilayer with the s and p polarized IR beam. Our ATR-FTIR results agree very well with those previously reported, with the amide I peak centered around 1644 cm^{-1} and amide II peak centered around 1454 cm^{-1} .^{28–30} The ratio of absorbance of the p and s IR beam at 1644 cm^{-1} is about 1.6. ATR-FTIR spectra of interfacial melittin can be fitted using one dominant peak centered around 1644 cm^{-1} . Below, we will combine both SFG and ATR-FTIR measurements to deduce the possible orientation distribution of melittin helices inside a bilayer.

Orientation Analysis. If melittin inside the DPPG bilayer indeed adopts a simple δ -distribution, the polarized ATR-FTIR measurement alone is sufficient to determine the only parameter required for a δ -distribution, the tilt angle. In the ATR-FTIR experiment, from the measured dichroic ratio of 1.6, the order parameter is calculated to be -0.075 . From such a value, the tilt angle is deduced to be 57.8° . Of course, the assumption of a δ -distribution may not be correct. Here, the order parameter is not very different from 0, from which little orientation information regarding the distribution can be deduced. If we consider that melittin is a bent α -helix, the measured ATR-FTIR amide I dichroic ratio alone cannot determine the tilt angle θ and the twist angle ψ simultaneously. The amide II dichroic ratio could provide additional information, but in practice the contribution of the HOD bending mode at 1450 cm^{-1} severely limits an analysis based on the amide II mode.

For a straight α -helix, SFG can provide two measurements, $\langle \cos \theta \rangle$ and $\langle \cos^3 \theta \rangle$. One common and simple way to deduce orientation parameters from SFG results is to use the intensity ratio of signals collected with different polarization combinations, such as ppp and ssp, to measure the ratio between $\langle \cos \theta \rangle$ and $\langle \cos^3 \theta \rangle$ and, thus, to determine θ . Figure 1 shows the correspondence of $|\chi_{zzz}/\chi_{yyz}|$ as a function of tilt angle θ_0 ,

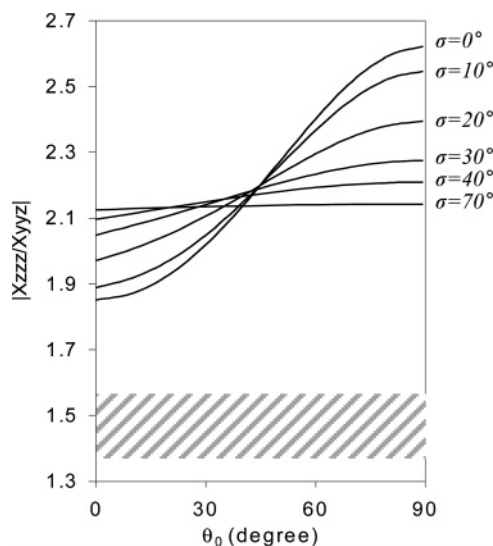


Figure 5. $|\chi_{zzz}/\chi_{yyz}|$ ratio as a function of orientation angle, assuming a δ -distribution or Gaussian distribution function. Shaded area represents the actual experimental result.

assuming a δ -function. If melittin adopts a δ -distribution, the $|\chi_{zzz}/\chi_{yyz}|$ value should be between 1.85 and 2.65. However in our SFG experiments, after fitting the spectra and considering Fresnel factors, the measured value is 1.4, below the possible range. This indicates that melittin does not adopt a δ -distribution.

Figure 5 displays the possible values of the $|\chi_{zzz}/\chi_{yyz}|$ ratio for Gaussian distributions with different widths. The possible values for Gaussian distributions are inside the possible range of the δ -distribution, indicating that melittin does not adopt a Gaussian distribution or a broader distribution that can be approximated by a Gaussian distribution. Therefore, assuming that melittin has an ideal α -helical structure, melittin's orientation at the concentration studied cannot be described by a simple single distribution function.

This prompts us to consider whether the bent structure of melittin can lead to a calculated $|\chi_{zzz}/\chi_{yyz}|$ value similar to the experimentally observed one. χ_{zzz} and χ_{yyz} are derived according to the method outlined above. Figure 6a and 6b show how $|\chi_{zzz}/\chi_{yyz}|$ changes as a function of θ and ψ in a 3-D plot and a contour plot, assuming a 135° interhelical angle θ_h . θ_h appears to be sensitive toward the environments, and other values of θ_h have also been reported in literature and are considered in the Supporting Information. It is clear that even after we consider the bent structure of melittin, the experimentally observed $|\chi_{zzz}/\chi_{yyz}|$ ratio cannot be achieved by assuming a single δ -distribution of θ and ψ . Only when an unreasonably small interhelical angle ($< 110^\circ$) is assumed can the theoretical calculation result approach the observed ratio, which should not be the real case. Therefore we believe that the bend alone does not explain the discrepancy between the experimental measurement and the possible orientation ranges described by a single δ -distribution or a Gaussian function.

Dual δ -Function. The inability of a single δ -function or Gaussian distribution to reproduce our experimentally observed intensity ratio prompts us to consider the next simplest distribution function, a dual δ -function. A dual Gaussian distribution will not be considered here because five parameters would be needed, which is currently beyond our ability to measure. As mentioned previously, a dual δ -function requires the determi-

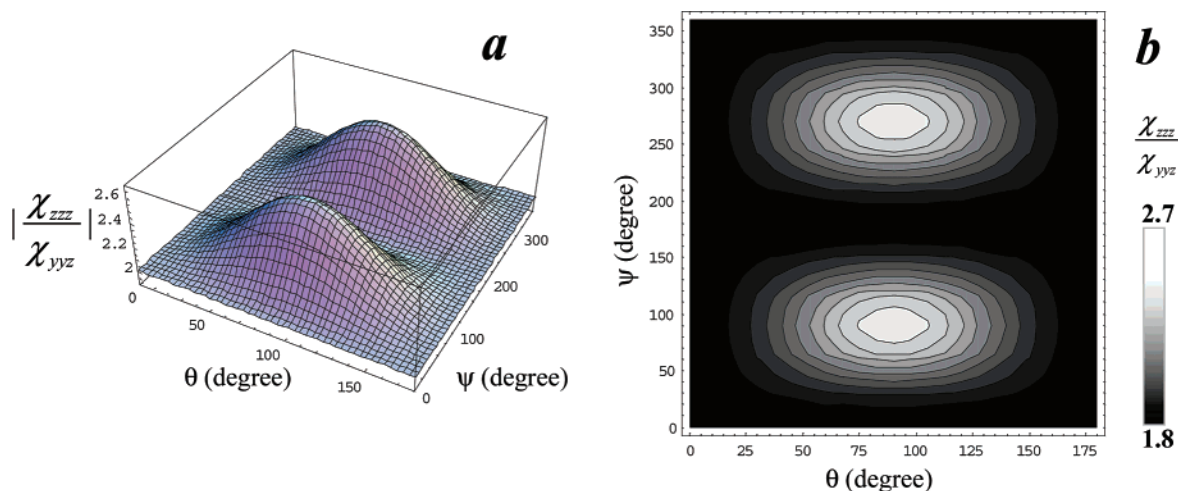


Figure 6. $|\chi_{zzz}/\chi_{yyz}|$ ratio as a function of orientation angle θ and ψ , assuming δ -distribution for both angles. (a) 3D plot and (b) contour plot with ratio represented by the gray scale.

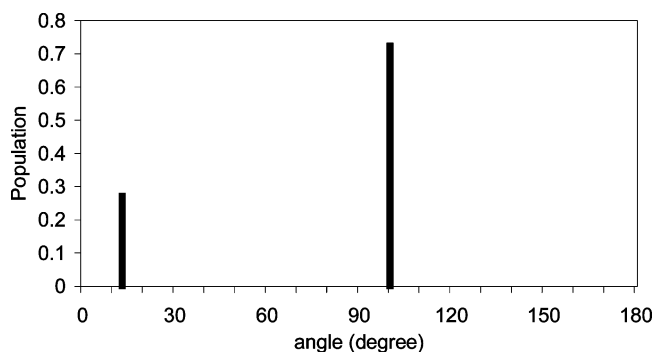


Figure 7. Orientation distribution derived based on a dual δ -distribution.

nation of three parameters: orientation angles θ_1 , θ_2 , and the population N_1 ($N_2 = 1 - N_1$). χ_{zzz} and χ_{yyz} can be calculated for each population based on their orientation, and the sum will be the total χ_{zzz} and χ_{yyz} of interfacial melittin.

Up to now, we have already obtained two equations, the first one involving $\langle \cos^2 \theta \rangle$ from the ATR-FTIR measurement, and the second one involving the ratio of $\langle \cos \theta \rangle / \langle \cos^3 \theta \rangle$ that is obtained from the SFG amide I ppp and ssp signal intensity ratio measurement. The third equation can be obtained from the SFG absolute intensity measurement, similar to the method utilized in several previous publications.³³

By calibrating the SFG absolute intensity of the amide I signal, we obtained the third equation which involves a linear combination of $\langle \cos \theta \rangle$ and $\langle \cos^3 \theta \rangle$. More details regarding the calculation can be found in the Supporting Information, and we have

$$\begin{aligned} \langle \cos \theta \rangle &= 0.139 = N \cos \theta_1 + (1 - N) \cos \theta_2; \\ \langle \cos^2 \theta \rangle &= 0.283 = N \cos^2 \theta_1 + (1 - N) \cos^2 \theta_2; \\ \langle \cos^3 \theta \rangle &= 0.248 = N \cos^3 \theta_1 + (1 - N) \cos^3 \theta_2. \end{aligned} \quad (7)$$

These three equations can be used to solve θ_1 , θ_2 , and N_1 . Only one valid solution to this set of equations is found, in which $\theta_1 = 13^\circ$, $\theta_2 = 100^\circ$, and $N_1 = 0.274$ ($N_2 = 0.726$). This would correspond to a scenario in which a quarter of melittin helices orient almost perpendicularly inside a lipid

bilayer, while the rest orient almost parallel to the bilayer surface (Figure 7). It is worth noting that these two types of melittin have opposite absolute orientations, and the destructive interference of SFG signals due to such opposite orientations leads to the small value of the observed $|\chi_{zzz}/\chi_{yyz}|$ ratio.

However, it should be pointed out that due to the complexity of the computation, the bent melittin structure is not considered in the above calculation. It is possible that the two populations may actually correspond to the two segments of a bent melittin molecule. We, however, believe this is not the case for the following reasons: First, the difference in the two orientation angles is less than 90° , and this would correspond to an “overly bent” structure of melittin. Second, the two orientations should have similar populations if they indeed come from the N-terminal and the C-terminal helices. Therefore we believe that melittin molecules in the lipid bilayer at the solution concentration tested here adopt two types of orientations.

Maximum Entropy. Maximum entropy has been shown to be the least biased approach in estimating distribution functions based on limited measurements.⁵⁰ The maximum entropy approach has been used in SFG studies to determine orientation distributions of the methyl group as well as the coiled coil structure in fibrinogen in our lab. The general form of a maximum entropy distribution is

$$G(\theta) = \exp - \sum_i \lambda_i \cos^i \theta \quad (8)$$

For the experiment with limited measurements, the general form has to be truncated to deduce the parameters in the function. If more measurements are available, the truncated function would more accurately represent the real distribution. In our combined ATR-FTIR and SFG studies, in addition to the normalization condition, three measured parameters can be obtained. Therefore overall four coefficients can be used to construct the distribution function

$$G(\theta) = \exp - (\lambda_0 + \lambda_1 \cos \theta + \lambda_2 \cos^2 \theta + \lambda_3 \cos^3 \theta) \quad (9)$$

Using the experimental results obtained, λ_1 , λ_2 , λ_3 , and λ_4 were calculated to be 0.4873, 18.3435, 38.2832, and -60.1843 ,

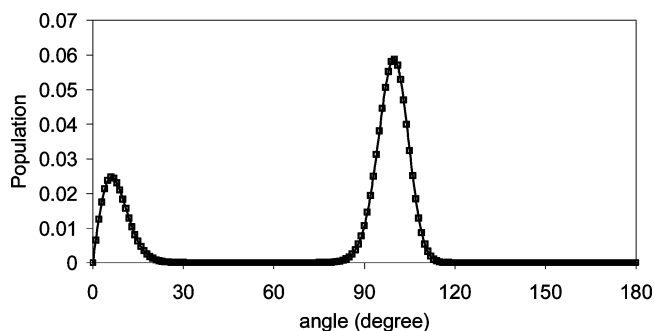


Figure 8. Orientation distribution derived based on the maximum entropy theory.

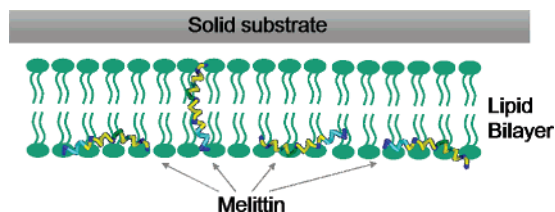


Figure 9. Schematic of the two orientations of melittin inside a lipid bilayer.

using a slightly modified Matlab program.⁵² The distribution based on maximum entropy theory is shown in Figure 8. It is important to note that we observe two local maxima in the distribution curve, one at about 6° and the other at about 100°, very similar to the results deduced by assuming a dual δ -function. We can also calculate the population of melittin adopting each orientation by integration since the orientation distribution function is normalized. The population of melittin molecules perpendicular and parallel to the bilayer surface is found to be 0.263 and 0.737, respectively. This again matches the population ratio obtained by assuming a dual δ -function. A schematic of the two orientations of melittin in a lipid bilayer is shown in Figure 9.

We believe that such an agreement between results obtained based on two distribution functions is not a coincidence. The small $|\chi_{zzz}/\chi_{yyz}|$ ratio is the underlying reason for the multiple distribution form of the solution. The two populations of melittin have their N \rightarrow C vectors orientated opposite to each other along the bilayer surface. Therefore the χ_{zzz} vector sum is effectively diminished, while the χ_{yyz} vector sum is less affected by such a configuration.

From the above analysis, it can be seen that melittin molecules interacting with a lipid bilayer, instead of orienting in a single direction, exist in different orientation states simultaneously. The maximum entropy function is a generic function, and no assumption of “two maxima” is included, but the resulting distribution is markedly similar to the assumed dual δ -distribution, which should represent the real distribution. According to such a distribution, we know that melittin adopts two kinds of orientation at the solution concentration we tested. This may correspond to the two distinct states of association with a lipid bilayer as described by the two-stage model. The orientation of a melittin helix reconstituted inside bilayers has previously

been studied by several techniques such as circular dichroism, ATR-FTIR, neutron reflection, and solid-state NMR. In most studies, only one dominant orientation of melittin is observed, probably due to the different experimental conditions (e.g., concentrations, the use of a premixed multi-bilayer/melittin system) and/or limitations on the measurements that can be obtained.^{21,24–28} It should be noted that magainin and alamethicin were shown to adopt two qualitatively distinct orientations previously.⁵³

Our results here demonstrate that combining SFG results with those obtained from linear vibrational spectroscopy (or other techniques in the future) leads to a greater number of measurable parameters, from which a more accurate orientation distribution can be deduced. The combined SFG and ATR-FTIR studies yield more reliable orientation information than the application of SFG or ATR-FTIR alone. More measurements can be obtained by using higher order nonlinear optical spectroscopic techniques such as four-wave mixing spectroscopy. In addition, isotope labeling of amino acid residues should provide many more measured parameters to deduce more accurate distribution functions. For SFG, isotope labeling not only shifts the vibrational frequency of the labeled species but also alters local inversion symmetry. Through careful design of a labeling strategy, it is possible to sequentially determine the orientation of every structural motif of a protein and thus obtain its coarse 3-D interfacial structure. When enough measurements are achieved in the experiments, a detailed orientation distribution can be deduced, even though such orientation information is sometimes complicated.

Conclusion

The vibrational spectroscopic nature of SFG allows structural investigation of both lipid bilayers and their interactions with proteins/peptides without exogenous labeling. We have combined SFG and ATR-FTIR results in this study and successfully deduced a more complicated orientation distribution of melittin, which we believe provides a better model for melittin/bilayer interactions. In this research, several possible distribution functions have been used to interpret the experimental results. Widely used single δ -function and single Gaussian distributions cannot reproduce observed amide I intensity ratios and, thus, cannot be used to describe melittin orientation distribution. A dual δ -function can match the experimental results, but such an assumption for the trial function needs further elaboration. A more generalized function with no particular assumptions, the maximum entropy function, has been used to fit the experimental results. Interestingly, the distribution so determined has two maxima and is very close to the dual δ -function. This strongly supports the idea that melittin helices exist in two main populations in the lipid bilayer at the solution concentration studied. About three-fourths of melittin molecules orient parallel to the bilayer surface with a slight tilt, while the rest orient more or less parallel to the surface normal. Such details have not been revealed before and cannot be deduced by SFG or ATR-FTIR alone. This work demonstrates the advantages of combining linear and nonlinear vibrational spectroscopy and the use of a maximum entropy function to deduce melittin

(52) Mohammad-Djafari, A. In *Maximum Entropy and Bayesian Methods*; Smith, C. R., Erickson, G., Neudorfer, P. O., Eds.; Kluwer Academic Publishers: Norwell, MA, 1992; Vol. 50, pp 221–234.

(53) Ludtke, S. J.; He, K.; Wu, Y.; Huang, H. W. *Biochim. Biophys. Acta, Biomembranes* **1994**, *1190*, 181–184.

orientation distribution. Similarly, this approach can be used to deduce orientations of α -helical secondary structures of membrane proteins to probe structural information of membrane proteins.

Acknowledgment. This work is supported by the Office of Naval Research (N00014-02-1-0832). X.C. thanks Eli Lilly for

a bioanalytical fellowship. Z.C. would like to acknowledge Dow Corning for the Dow Corning Professorship.

Supporting Information Available: Details about the experiments, hyperpolarizability calculation for a bent helix, and deduction of $\langle \cos \theta \rangle$, $\langle \cos^2 \theta \rangle$, and $\langle \cos^3 \theta \rangle$. This material is available free of charge via the Internet at <http://pubs.acs.org>.

JA067446L